Reflection of Rydberg antihydrogen by surfaces

D. Comparat ⬤

Université Paris-Saclay, CNRS, Laboratoire Aimé Cotton, 91405, Orsay, France

We study Rydberg antihydrogen interaction with a metallic or dielectric surface by calculating the adiabatic potential curves. For a metallic or pure dielectric surface with permittivity $\epsilon = \infty$, the image charges create an attractive potential that pulls the positron away from the antiproton when the atom approaches the surface. This is no longer the case with low-dielectric-constant materials ($\epsilon \approx 1$). Furthermore, using a negative positron work function, meaning that positrons are repelled by these surfaces, only repulsive potential curves exists. This suggests that Rydberg antihydrogen can probably be repelled by such ultralow-k materials, opening the way for simple manipulation and guiding of antimatter (antihydrogen or positronium) systems.

I. INTRODUCTION

Collision of an antimatter system with a matter surface is widely believed to lead to annihilation. However, it is well known that positron can be repelled by some materials because of an existing negative work function. This suggests the possibility for antimatter systems containing positrons, such as antihydrogen or positronium, to be repelled by a surface. This is an appealing method to manipulate antiatoms such as antihydrogen ($\overline{\text{H}}$) that are routinely produced at CERN's Antiproton Decelerator in a broad range of Rydberg states [1]. This is very similar to what has been suggested for Rydberg matter atoms: reflection from a liquid helium surface (that has a negative work function for electrons) [2,3]. In our paper, we rephrase the arguments for an antimatter system and calculate more precisely the potential interaction curves. We stress that this reflection occurs because of a repulsive potential and thus has nothing to do with the so-called quantum reflection phenomenon, also proposed for antihydrogen [4], which is a quantum and counterintuitive phenomenon where the motion of slow particles is reverted even in the presence of an attractive potential.

We first briefly discuss the positron interaction with a metallic or dielectric surface with permittivity ϵ to get a simple intuitive picture and a simplified interaction potential. Then we diagonalize the electronic (here leptonic, in fact) Hamiltonian to get the potential interaction curve of an antihydrogen atom at a distance Z of a surface. Finally, based on simple adiabatic considerations, we suggest that, independent of its internal state, almost all Rydberg antihydrogen atoms can be repelled by material with a negative work function that is acting as a positron repeller—the main condition being that no attractive charge image potential exists with a low permittivity $\epsilon \approx 1$ material. We finally briefly discuss the annihilation and magnetic-field effects and then conclude by discussing interest in antihydrogen or positronium experiments.

II. ELECTRON-POSITRON AND SURFACE

Interaction of positrons with atoms, molecules, and surfaces is a very rich topic that has been studied quite extensively (see, for instance, Refs. [5–7]), especially for its usefulness for defect studies using positron annihilation [8]. Positron interactions differ from electron ones, at least from the charge and Pauli's exclusion principle point of view, leading to major consequences, for instance, for surface diffraction experiments, such as in total-reflection high-energy positron diffraction (TRHEPD), which is the positron counterpart of reflection high-energy electron diffraction (RHEED). A very illustrative example of the difference between electron and positron is given by the work function $\Phi^{\pm}$, where $^+$ denotes the positron case and $^-$ the electron one. The work function is the sum of two terms: the bulk chemical potential $\mu^{\pm}$ and the surface dipole potential: $\Phi^{\pm} = \mp\Delta - \mu^{\pm}$. The interesting fact is that, because of the positron's opposite charge compared to the electron, the surface dipole potential barrier (Δ that typically prevent electrons to escape form the bulk) has the reverse effect on positrons than on electrons. We thus see that if Δ is large enough to overcome the positron chemical potential, the positron work function Φ^+ can be negative [9]. This occurs if the positron ground state lies higher in energy than the vacuum level, and so positrons may spontaneously be (re)emitted from the surface of the bulk material. For this reason, metals such as W or Pt are used as positron moderators.

The fact that positron can be repelled by a surface is the first key parameter we are going to use. The second key parameter is the long-range interaction between the material and the positron (and also obviously the antiproton). In the well-known electron case, when an electron ($-e$ charge) is extracted from a metal toward the vacuum at distance z, a $+e$ image charge (hole) is created in the metal that screens exactly the electric field generated by the electron at the metal surface (at $z = 0$). The electric field $E(z)$ generated by the charge image (hole) acting on the electron is: $E(z) = \frac{e}{4\pi\varepsilon_0(2z)^2}$ and
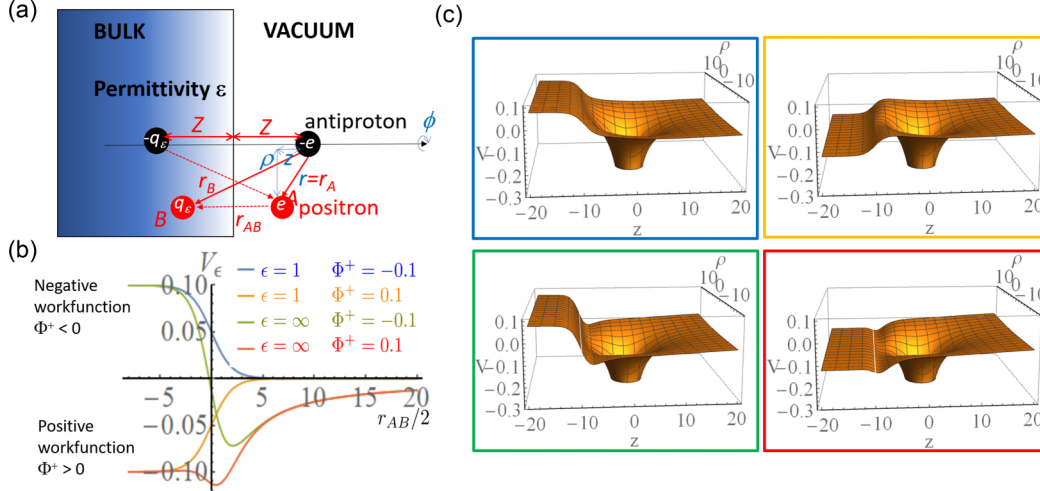
FIG. 1. Interaction potential seen by the antihydrogen system. (a) Notation of the distance between particles, and their image charges. (b) Positron interaction potential V_ϵ with the surface. The two extreme cases of a metal or a perfect dielectric ($\epsilon = \infty$), and of an ultralow-dielectric-constant (low-k) materials ($\epsilon \approx 1$) are illustrated, as well as the two cases of positive and negative work functions. (c) Total potential V drawn in the same extreme cases from top to bottom: $\epsilon = 1(\Phi^+ = -0.1, \Phi^+ = 0.1)$, $\epsilon = \infty(\Phi^+ = -0.1, \Phi^+ = 0.1)$. Values are given in atomic units.

the associated potential energy is $V_{\text{image potential}}(z) = -\frac{e}{4\pi \varepsilon_0 (4z)}$. The exact same discussion occurs for positrons with the exact same result for a metal or for a perfect dielectric (that is with permittivity $\epsilon = \infty$). In the more general case of a more realistic dielectric media, with a dielectric constant ϵ, the image charge is not exactly opposite to the real charge but is given by $q = q_\epsilon = -\frac{\epsilon - 1}{\epsilon + 1} e$.

It is way beyond the scope of this paper to deal with the overall complexity of the full positron interaction potential, especially near a surface (metallic, semiconductor [10], dielectric, or even heterostructure or with multilayer coating [11]) that depends on many physical aspects such as the electronic band (gap) structure, the electron (or positron [12]) affinity, Fermi level and positronium formation potential. Our goal is to use simple models to identify the key behaviors and trends. Thus, we will simplify the problem of the positron interaction potential with a material by using, as discussed previously, an effective work-function parameter such that $-\Phi^+$ defines the barrier height between the vacuum and the surface, as shown in Fig. 1(b). Because the charge image model is valid only asymptotically, i.e., for a positron-surface distance z_p that is a few Bohrs away from the image plane [13,14], we smoothed this border to avoid corrugation effects along the surface, using a β parameter (for all numerical applications, we use $\beta = 1a_0$ value).

So, in summary, our simple positron interaction potential with the surface will be modeled by

$$V_\epsilon[z_p] = \frac{q_\epsilon}{4\pi \varepsilon_0} \frac{1}{4z_p} \frac{1 - e^{-\beta z_p}}{(1 + e^{-\beta z_p})^2} - \Phi^+ \frac{1}{1 + e^{\beta z_p}}. \quad (1)$$

This formula, inspired by the one given in Ref. [15], has no physical ground, except interpolating simply and smoothly between the regions far from the surface. The two extreme cases of a metal or a perfect dielectric, ($\epsilon = \infty$, $q_\epsilon = -e$), and of ultralow-dielectric-constant (low-k) materials ($\epsilon \approx 1$, $q_\epsilon = 0$) are illustrated in Figs. 1(b) and 1(c).

III. INTERACTION OF RYDBERG ANTIHYDROGEN WITH SURFACES

Interaction of Rydberg atoms with surfaces has a long history (for a review, see Ref. [16]). The interaction can be divided in long range (where the distance between the Rydbergs is larger than the Rydberg radius) and short range where surface effects such as work function plays a role. Due to the charge images [cf. Fig. 1(a)], the problem is very similar to H_2, H_2^+, or even $H - \bar{H}$ interactions [17–19], especially in Rydberg states [20,21]. We will treat the problem assuming first the Born-Oppenheimer approximation, which is with a fixed position of the heavy particle (antiproton and its image).

A. Hamiltonian and interaction potential

The notations are given in Fig. 1(a) with Z the distance between the antiproton and the surface, $\boldsymbol{R}$ the vector position of the antiproton (of mass M), and $\boldsymbol{R} + \boldsymbol{r}_A$ the vector position of the positron (of mass m). $r = r_A$ is the distance between the antiproton and the positron (A), r_B the distance between the antiproton and the charge image of the positron (B), and $z_p = r_{AB}/2$ the distance between the positron and the surface.

We neglect relativistic effects such as the nuclear and electron spins or Casimir Polder-retardation in the electromagnetic interaction. So the electrostatic potential is given by [22]

$$V = \frac{e}{4\pi \varepsilon_0} \left[\frac{q_\epsilon}{4Z} - \frac{e}{r_A} - \frac{q_\epsilon}{r_B} \right] + eV_\epsilon[r_{AB}/2]. \quad (2)$$

The kinetic energy is given by

$$H_{\text{kin}} = -\frac{\hbar^2}{2M} \nabla_{\boldsymbol{R}}^2 - \frac{\hbar^2}{2\mu} \nabla_{\boldsymbol{r}_A}^2 + \frac{\hbar^2}{M} \nabla_{\boldsymbol{r}_A} . \nabla_{\boldsymbol{R}},$$

where $\mu = \frac{mM}{m+M}$ is the reduced mass of the (anti)hydrogen system and the third term (so-called mass polarization term) couples antiproton and positron motions.

We start with the adiabatic-Born Oppenheimer approximation that is looking for product wave function $\Psi(\boldsymbol{r}_A, \boldsymbol{r}_B, \boldsymbol{R}) = \Psi_n(\boldsymbol{R})\Psi_e(\boldsymbol{r}_A, \boldsymbol{r}_B, Z)$ of a nuclei (n) part (we keep here this terminology even if hadronic in fact) and an electronic (e) (here leptonic) part. The electronic wave function satisfies the Schrödinger equation:

$$\left[-\frac{\hbar^2}{2\mu}\nabla_{\boldsymbol{r}_A}^2 + V \right]\Psi_e = V_e\Psi_e. \tag{3}$$

Therefore, for a given Z, we solve the Schrödinger equation, the solution of which defines the electronic potential $V_e(Z)$ under which the nuclear part evolves (if neglecting the mass separation term).

B. Lagrange-mesh method and generalized Gauss Laguerre quadrature

Following Refs. [23,24], we use the Lagrange-mesh method [25,26] to find $V_e(Z)$ from Eq. (3).

A method to find the proper coordinate system is given in Refs. [27,28] and we use here the scaled parabolic coordinates $u = \lambda(r + z) = \lambda\eta > 0$, $v = \lambda(r - z) = \lambda\xi > 0$, and ϕ [defined from the cylindrical coordinates (z, ρ, ϕ) cf. Fig. 1(a)].

The system has axial symmetry around the internuclear z axis. Therefore, we can immediately write the electronic wave function as $\Psi_e(\xi, \eta, \phi) \propto e^{im\phi}$ where m is the projection of the positron angular momentum on the z axis. Using atomic units (in fact, slightly modified because μ is not exactly m_e) that is, roughly speaking $\hbar = \mu = \frac{e^2}{4\pi\varepsilon_0} = 1$, Eq. (3) becomes $[\hat{T} + V - V_e]\Psi_e = 0$, with

$$\hat{T} = -\frac{1}{2}\nabla_{\boldsymbol{r}_A}^2 = \frac{2\lambda^2}{u+v}\left\{ -\frac{\partial}{\partial u}\left[u\frac{\partial}{\partial u} \right] \right.$$
$$\left. -\frac{\partial}{\partial v}\left[v\frac{\partial}{\partial v} \right] + \frac{m^2}{4}\left(\frac{1}{u} + \frac{1}{v} \right) \right\}, \tag{4}$$

and V, cf. Eq. (2), can be expressed in u, v coordinates, using:

$$r_A = r = \frac{u+v}{2\lambda},$$
$$\frac{r_{AB}}{2} = Z + z = Z + \frac{u-v}{2\lambda},$$
$$r_B = \sqrt{-\frac{(u-v)^2}{4\lambda^2} + \frac{(u+v)^2}{4\lambda^2} + \left(Z + \left| Z + \frac{u-v}{2\lambda} \right| \right)^2}.$$

The absolute value arises because if $Z + z < 0$ the positron is inside the bulk.

Because the Stark hydrogen wave function is expressed in terms of the orthonormal functions $\varphi_n(x) = \left[\frac{n!}{(n+|m|)!} \right]^{1/2} L_n^{|m|}(x) x^{|m|/2} e^{-x/2}$ [29] (for $x = \xi/n$ or $x = \eta/n$), it is intuitive, for our problem of an antihydrogen atom under the field of the image charges, to use discrete-variable-representation (DVR) method related to the Lagrange-mesh method. If the optimal choice for λ can be obtained by minimizing as many of the lowest eigenvalues as possible, the scaled Stark hydrogen wave function already indicates that typically $\lambda \sim 2/n$, for the study near the principal quantum number n of interest, is a good choice [26].

We use a Gauss-quadrature approximation at the zeros x_i, for $i = 1, \ldots, N$, of the generalized Laguerre polynomial

of order N ($L_N^{|m|}(x_i) = 0$). This leads to the grid point $u_i = x_i$ and $v_j = x_j$ and the one-dimensional Lagrange (DVR) basis functions [23,30,31] $f_i(u) = w_i^{1/2}\sum_{n=0}^{N-1}\varphi_n(u_i)\varphi_n(u)$— that is, $f_i(x) = (-1)^i x_i^{1/2}(\frac{(N+|m|)!}{N!})^{-1/2}\frac{L_N^{|m|}(x)}{x-x_i}x^{|m|/2}e^{-x/2}$ with the weight $w_i = \frac{1}{x_i(\varphi_N'(x_i))^2} = \frac{(N+|m|-1)!e^{x_i}}{N!(N+|m|)x_i^{|m|-1}(L_{N-1}^{|m|}(x_i))^2}$ such that $f_i(u_j) = w_i^{-1/2}\delta_{ij}$ and $\int_0^\infty f_i(u)f_j(u)du = \delta_{ij}$. Taking care of the Jacobian from the coordinate transformation ($d^2\boldsymbol{r} = \rho d\rho dz = \frac{u+v}{4\lambda^3}dudv$), the two-dimensional Lagrange basis is formed from a direct product of one-dimensional bases $f_{ij}(u, v) = [\frac{u+v}{4\lambda^3}]^{-1/2}f_i(u)f_j(v)$. The pseudospectral method, or DVR (Laguerre mesh) basic approximation, is then the fact that a normalized function $\chi(u, v)$ ($\int d^2\boldsymbol{r}|\chi|^2 = 1$) is approximated by $\chi(u, v) \approx \sum_{ij}f_{ij}(u, v)\chi_{i,j}$ with $\chi_{\alpha=\{i,j\}}$ being a unitary vector. Thus, because of the Jacobian coordinate transformation, the wave function $\chi(u, v)$ is represented by a (normalized) vector whose components are given by $\chi_{i,j} = [\frac{(u_i+v_j)w_i w_j}{4\lambda^3}]^{1/2}\chi(u_i, v_j)$ where w_i is the weight related to the Gauss-Laguerre quadrature points.

In summary, the overall information is thus discretized at a few grid points. We use the approximation of the substitution of the exact integration by the two-dimensional quadrature formula $\int_0^\infty du \int_0^\infty dv g(u, v) \approx \sum_{i=1}^N w_i \sum_{j=1}^N w_j g(u_i, v_j)$. In our case, all potential and kinetic information is thus discretized. We note $V_{ij,i'j'} = V(u_i, v_j)\delta_{ii'}\delta_{jj'}$ and $T_{ij,i'j'} = \int_0^\infty du \int_0^\infty dv f_{ij}(u, v)\hat{T}f_{i'j'}(u, v)$ is given by

$$T_{ij,i'j'} = 2\lambda^2 \frac{t_{ii'}\delta_{jj'} + t_{jj'}\delta_{ii'}}{(u_i + v_j)^{1/2}(u_{i'} + v_{j'})^{1/2}},$$

where

$$t_{ii} = \frac{1}{3}\left(N - \frac{u_i}{4} + \frac{m^2 - 1}{2u_i} + \frac{|m| + 1}{2} \right),$$

and for $i' \neq i$,

$$t_{ii'} = \frac{2(-1)^{i-i'}(u_i u_{i'})^{1/2}}{(u_i - u_{i'})^2}.$$

This exact evaluation of the kinetic energy term is a very useful property because the highly singular numerical derivatives are avoided, which is not the case with most of the other numerical methods based on propagation on a grid. The DVR also makes possible the inclusion of a realistic potential since we only need the wave function at the grid points, thereby avoiding the singularity at the origin. Finally, the matrix elements $T_{ij,i'j'}$ of the kinetic energy term need to be evaluated only once for a particular symmetry of the problem, so changing the potential is straightforward.

To be able to treat the positron escape, we have to deal with continuum states. So, we will use the complex scaling rotation methods ($\boldsymbol{r} \rightarrow \boldsymbol{r}e^{i\theta}$) in which the continuum states appear now as square integrable and vanish asymptotically. So, in summary, we have the discrete Hamiltonian [30,31]:

$$H_{ij,i'j'} = e^{-2i\theta}2\lambda^2 \frac{t_{ii'}\delta_{jj'} + t_{jj'}\delta_{ii'}}{(u_i + v_j)^{1/2}(u_{i'} + v_{j'})^{1/2}}$$
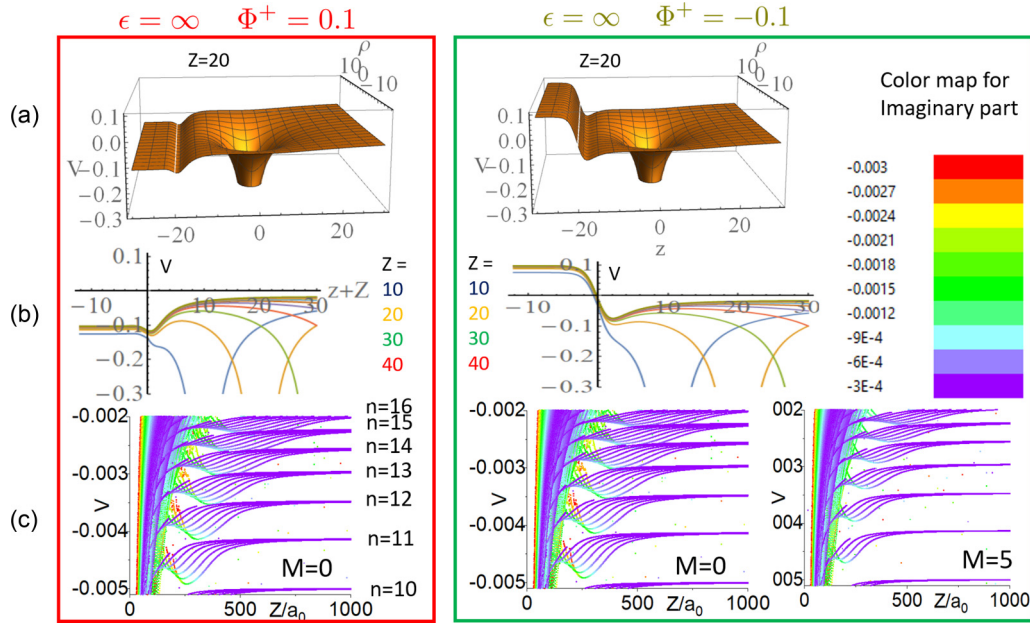$$+ V(u_i e^{i\theta}, v_j e^{i\theta})\delta_{ii'}\delta_{jj'}. \tag{5}$$

FIG. 2. (a), (b) Positron interaction potential V_ϵ with the surface for an antihydrogen atom at distance Z of a metal or a perfect dielectric ($\epsilon = \infty$) material. $Z = 20\, a_0$ in (a) and Z varies from $10a_0$ to $40a_0$ in (b) where only the pure axial ($\rho = 0$) potential is shown. The interaction potentials are given for a positive (left-red box) and negative (green-right box) work function (of ± 0.1 atomic units). (c) Potential curve of the antihydrogen atom in function of Z in these two cases and for angular momentum $m = 0, 5$ in the energy region of $n = 10 - 16$.

Equation (5) defines a Hamiltonian matrix of size $N^2 \times N^2$. The potential energy matrix is diagonal and eigenvalues from the diagonalization of the Hamiltonian matrix directly give the energies. They are plotted in Figs. 2 and 3. More precisely, because of the complex scaling rotation methods, real and imaginary parts of the eigenvalues correspond, respectively, to the energies and half widths ($\Gamma/2$) of the resonance states. We generally choose the complex scaling angle as a convergence parameter, such that the eigenvalues do not vary with small changes in the rotation angle. We find $\theta \approx 0.4$ convenient for

our cases (but when no continuum state is present, $\theta = 0$ is obviously a good choice).

C. Potential curves

Lagrange mesh points x_i and diagonalization of Eq. (5) are straightforwardly calculated using MATHEMATICA software and we present results for states between $n = 10$ and $n = 16$. This choice is convenient to avoid plotting too many curves and are already well representative of Rydberg behavior. From such plots, it is quite easy to extrapolate to higher levels because of a clear n scaling dependence. For such a region, $N = 50$ grid points are enough to get a very decent picture but we choose $N = 70$ (and step $1a_0$ for Z) for the plots. Other parameters are $\lambda = 0.1, \theta = 0.4, \phi^+ = \pm 0.1$.
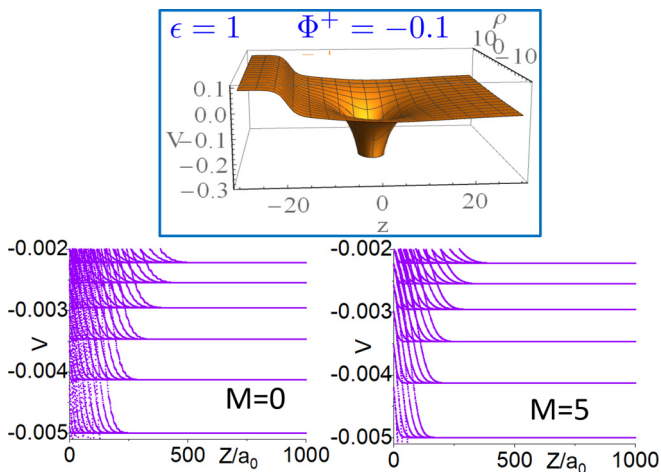

FIG. 3. Interaction potential (upper part) and adiabatic potential curves (lower part) of an antihydrogen atom at distance Z from an ultralow-dielectric-constant (low-k) material ($\epsilon \approx 1$) with a negative positron work function. The cases of angular momentum $m = 0, 5$ are shown.

D. Metallic or perfect dielectric surface: $\epsilon = \infty$

We first present in Fig. 2 the interaction of an antihydrogen atom with a metallic or perfect dielectric surface, that is, with a surface having $\epsilon = \infty$. Because of the $1/4Z$ [in atomic units, cf. Eq. (2)] interaction potential due to the antiproton with its image charge, all potential curves are attractive and lead to unstable states. This arises independently of the value of the work function because the potential barrier on the surface side of the antiproton becomes lower and thinner, thus enhancing the ionization. This is clearly visible in Fig. 2(b), where the potential has a saddle point along the z axis (for $\rho = 0$) between the antiproton and the surface. The process is thus absolutely identical to the one of hydrogen atoms approaching a metallic surface. This has been studied extensively (see Ref. [16] and references therein) and the results are indeed the destruction of the Rybderg. We note that the potential curves show characteristics that are similar to the

pure Stark states with lower energy redshifted (respectively, higher energy blueshifted) states with the induced atomic dipole moment, p, parallel (respectively, antiparallel) to the image charge field, E, and the associated potential energy, $-p.E$, negative (respectively, positive). Therefore blueshifted stark states would ionized at lower fields, meaning closer to the surface, than the redshifted states because the dipole orientation indicates that for blue states the positron location is mainly in an opposite position of the saddle point and thus, classically speaking, it is harder for the positron trajectory to find the way to this saddle point. However, once the saddle point passed, the motion along ρ is free and the positron is removed from the antiproton and is likely to be lost. The value of the work function is only here to determine the future of this free positron which can either be annihilated, trapped in a surface state which, together with an electron, might also form positronium, or be backscattered. Depending on the initial state, the followed potential curves might be different, but for us the important net result is the Rydberg destruction when approaching the surface. We could have thought that a sort of centrifugal barrier could have prevented this effect but high m states have a similar behavior as shown in Fig. 2, with similar behaviors for $m = 0$ and $m = 5$ cases.

E. Low-k material $\epsilon = 1$

In low-k material, the image charge is reduced and even absent for the limiting case of $\epsilon = 1$. We can thus expect a totally different behavior. With no charge image, the Rydberg atoms moves freely until the positron approaches the surface layer. Clearly, with a positive work function, the potential of Fig. 1 indicates that the positron will be caught by the surface and thus probably will annihilate, leading to the destruction of the Rydberg atoms. Thus, the only interesting case is the one with a negative work function, shown in Fig 3.

Because of the negative work function, the positron is repelled from the surface. This always leads, for the Rybderg atom, to repulsive potential curves. The states are bound and so calculus is performed with $\theta = 0$.

F. Simple adiabatic consideration for the reflection on surface.

If the curves are repulsives, we can expect reflection of the antihydrogen during its motion. However, this relies on adiabatic (Born-Oppenheimer) curves. We would like to check this assumption for antihydrogen as produced in experiments. In typical antihydrogen experiments at CERN, the Rydberg $n = 20 - 60$ are formed at temperatures of ~ 40 K or slightly higher [1] so with velocities in the $v_\perp \sim 1000$ m/s range. When approaching (at orthogonal velocity $v_\perp$) the surface, the characteristic time of atom-surface interaction $\sim a_0 n^2 / v_\perp$ (in the 0.1 ns range), given by the Rydberg size divided by the velocity, is much longer than the orbital period of Rydberg electron $2n^2 h / E_h$ (in the ps range), where $E_h = 4.36 \times 10^{-18}$ J is the atomic units for energy. We might thus expect adiabatic following of the potential curves. This assumption was used in Refs. [2,3] to study Rydberg hydrogen approaching a He surface. The authors even further simplify the problem by assuming a sharp infinite repulsive potential curve ($\beta = 0$, $\Phi^+ = -\infty$) to be able to solve analytically the

problem in ellipsoidal coordinates. Limiting cases correspond first to paraboloidal coordinates, as Z tends to infinity—so for the initial Stark state $|n, n_1 = n_\xi, n_2 = n_\eta, m\rangle$ (with $n = n_\xi + n_\eta + |m| - 1$ and n_ξ, n_η positives)—and, second, to spherical polar coordinates, as Z tends to zero, that is, when the (anti)proton hits the surface with a Rydberg state $|n'l'm'\rangle$. The adiabatic link is provided, as in H_2^+ [32], by $n' = n_\xi + 2n_\eta + |m| + 2$, $l' = 2n_\eta + |m| + 1$, $m' = m$. The condition for the reflection of the Rydberg atoms from the surface is thus simply a kinetic energy insufficient to climb the energy difference: $\frac{1}{2} M v_\perp^2 \leqslant \frac{E_h}{2}(\frac{1}{n^2} - \frac{1}{n'^2})$. $n < n' = n + n_\eta + 1$ is always verified, so the worst case is $n' = n + 1$. In such a case, the critical velocity is thus 400 m/s for $n = 30$. This is similar to antihydrogen velocities produced in experiments. For colder antihydrogen (<20 K), the initial velocity will even be smaller and atoms will always be reflected from the surface. To have a better understanding of the adiabatic versus nonadiabatic behavior, we would need a more complex charge transfer dynamics that would be extremely difficult to carry for $n > 20$ states [33]. But, this simple adiabatic picture already gives interesting results. However, care has to be taken because the potential height is not infinite in our case and is modified by the value of the work function. Furthermore, it is well known than nonadiabatic effects play a significant role in Rydberg-anti Rydberg or Rydberg surface interactions [16,21,33]. However, our realistic potential curves shows similar behaviors than the simple analytical model of Refs. [2,3] with always repulsive curves and, because we find that all potential curves are repulsive, we can safely ensure a total reflection for slow antihydrogen atoms as formed in current experiments at CERN.

IV. CONCLUSION

We found that, as for hydrogen, Rydberg antihydrogen interaction with a metallic surface (or surface with high permittivity) will lead to ionization due to the attractive image charge effect and thus independently of the sign of the positron work function. The first important result is thus that positron repulsion does not ensure antihydrogen reflection. Thus, evidence of a high reflection coefficient (of 0.58 [34]) for very low-energy (20 eV) positrons on tungsten surfaces does not mean that Rybderg antihydrogen will be reflected from a W surface even if the work function of W (110) foil is -3.0 eV and that of W (100) is -2.48 eV.

However, for low-permittivity material, the attraction does not exist anymore and if, in addition, the surface repels positrons, we expect classical reflection of the antihydrogen from the surface. It is beyond the scope of this paper to study in detail the material properties, but it is obviously crucial to know that such material exists or are in current development (cf. Ref. [35] and reference therein for a comparison of dielectric constants of various materials). Some of them are based on positron moderators (that thus repelled positrons); one of the simplest examples being solid neon, well known as a positron moderator for producing slow positrons with $\epsilon = 1.24$ [36–39]. Because they are used as positron moderators, the annihilation would be practically absent during (at longest) nanosecond range interaction time between the Rydberg and the surface [40]. We take the opportunity to

mention here that solid neon can also be a very good choice to reflect Rydberg positronium. We did not study the case of Rydberg positronium here but, because solid neon repels positrons as well as electrons, it will, quite probably, repel Rydberg positronium, such as many of other materials [41–43]. Other low-k materials are in development either based on silicon oxide derivatives (SiO_2 has $k = \epsilon = 4$), organic compounds, aerogels, or mesoporous systems with one recent quite ideal example of amorphous boron nitride films with ultralow values of $\epsilon = 1.16$ at 1 MHz frequency and probably even lower at higher frequency such as the one present in our Rybderg-surface interaction case (the frequency being in the GHz region = inverse of the typical interaction time) [35].

We did not treat the case of a magnetic field, often present in some antihydrogen experiments. It is easy to treat the case of a magnetic field B along the z axis by simply adding the linear $m\frac{B}{2}$ and quadratic $\frac{B^2}{8}\rho^2 = \frac{B^2}{8}\frac{uv}{\lambda^2}$ Zeeman terms in the potential, where B is the value in atomic units (2.35×10^5 T). The resulting potential curves are almost indistinguishable from the ones (cf. Fig. 2) without magnetic field. However,

this case of magnetic field orthogonal to the electrodes is not the most common one, and more complex (3D grids and no separation in m values) calculations would be needed to treat the general case. It can be done but it will probably not change much the case of low-k materials without image charge effect. But, in other cases, magnetic field can even help for antihydrogen reflection in the case of a metallic surface interaction because of the complex energy-level structure that can, thanks to avoided crossing, limit a too strong acceleration produced by the antiproton image charge.

We hope that our study will trigger more detailed theoretical and experimental investigations to provide efficient Rydberg antihydrogen, or positronium, surface reflection that could be quite useful for transporting or focusing a beam, for instance, for a gravity measurement [1,44–46].

[1] M. Charlton, S. Eriksson, and G. M. Shore, Testing fundamental physics in antihydrogen experiments, arXiv:2002.09348 (2020).

[2] P. B. Lerner and I. M. Sokolov, Rydberg atom at the surface of liquid helium, Zh. Eksp. Teor. Fiz. **44**, 501 (1986) [JETP Lett. **44**, 644 (1986)].

[3] S. K. Sekatskii, On the reflection of Rydberg atoms from a liquid helium surface, Z. Phys. D: At. Mol. Clusters **35**, 225 (1995).

[4] Gabriel Dufour, A. Gérardin, R. Guérout, A. Lambrecht, V. V. Nesvizhevsky, S. Reynaud, and A. Yu. Voronin, Quantum reflection of antihydrogen from the Casimir potential above matter slabs, Phys. Rev. A **87**, 012901 (2013).

[5] P. J. Schultz and K. G. Lynn, Interaction of positron beams with surfaces, thin films, and interfaces, Rev. Mod. Phys. **60**, 701 (1988).

[6] C. M. Surko, G. F. Gribakin, and S. J. Buckman, Low-energy positron interactions with atoms and molecules, J. Phys. B: At., Mol. Opt. Phys. **38**, R57 (2005).

[7] C. Hugenschmidt, Positrons in surface physics, Surf. Sci. Rep. **71**, 547 (2016).

[8] R. Krause-Rehberg and H. S. Leipner, *Positron Annihilation in Semiconductors: Defect Studies* (Springer-Verlag, Berlin, 1999), Vol. 127.

[9] R. M. Nieminen and C. H. Hodges, Positron work functions in transition metals, Solid State Commun. **18**, 1115 (1976).

[10] N. Bouarissa, B. Abbar, J. P. Dufour, N. Amrane, and H. Aourag, Work function and energy levels of positrons in elemental semiconductors, Mater. Chem. Phys. **44**, 267 (1996).

[11] V. V. Pogosov, A. V. Babich, P. V. Vakula, and A. G. Kravtsova, On the positron work function for a metal with a dielectric coating, Tech. Phys. **56**, 1689 (2011).

[12] M. J. Puska, P. Lanki, and R. M. Nieminen, Positron affinities for elemental metals, J. Phys.: Condens. Matter **1**, 6081 (1989).

[13] N. D. Lang and Walter Kohn, Theory of metal surfaces: Induced surface charge and image potential, Phys. Rev. B **7**, 3541 (1973).

[14] A. V. Babich, P. V. Vakula, and V. V. Pogosov, To the problem of positron states in metal-insulator nanosandwiches, Phys. Solid State **57**, 142 (2015).

[15] P. A. Serena, J. M. Soler, and N. Garcia, Self-consistent image potential in a metal surface, Phys. Rev. B **34**, 6767 (1986).

[16] M. W. Kohlhoff, Interaction of Rydberg atoms with surfaces, Eur. Phys. J.: Spec. Top. **225**, 3061 (2016).

[17] B. R. Junker and J. N. Bardsley, Hydrogen-Antihydrogen Interactions, Phys. Rev. Lett. **28**, 1227 (1972).

[18] W. Kolos, D. L. Morgan Jr., D. M. Schrader, and L. Wolniewicz, Hydrogen-antihydrogen interactions, Phys. Rev. A **11**, 1792 (1975).

[19] P. Froelich, S. Jonsell, A. Saenz, B. Zygelman, and A. Dalgarno, Hydrogen-Antihydrogen Collisions, Phys. Rev. Lett. **84**, 4577 (2000).

[20] A. Yu. Voronin and J. Carbonell, Hydrogen–antihydrogen atomic interaction at subkelvin temperatures, Nucl. Instrum. Methods Phys. Res., Sect. B **214**, 139 (2004).

[21] V. Sharipov, L. Labzowsky, and G. Plunien, Rydberg states of the hydrogen-antihydrogen quasimolecule, Phys. Rev. A **73**, 052503 (2006).

[22] The charge image methods solve the problem for the electric field, not for the potential. So some care has to be taken for calculating the potential, that is, the time derivative of which leads to the proper Newton's equations. Care also has to be taken when the positron is inside the material because obviously its image charge does not exist anymore. Fortunately, we will use only the $\epsilon = 1$ and $\epsilon = \infty$ cases that are simple.

[23] D. Dimitrovski, Time-dependence of ionization and excitation by intense, short electric pulses, Ph.D. thesis, Fakultät für Math-

ematik und Physik, Freiburg, Germany, 2005, https://freidok.uni-freiburg.de/data/1888.

[24] E. So, Interaction of Rydberg hydrogen atoms with metal surfaces, Ph.D. thesis, Oxford University, UK, 2011.

[25] D. Baye, Lagrange-mesh method for quantum-mechanical problems, Phys. Status Solidi (b) **243**, 1095 (2006).

[26] D. Baye, The lagrange-mesh method, Phys. Rep. **565**, 1 (2015).

[27] C. Waksjö and S. Rauch-Wojciechowski, How to find separation coordinates for the Hamilton-Jacobi equation: A criterion of separability for natural Hamiltonian systems, Math. Phys., Anal. Geom. **6**, 301 (2003).

[28] Yu. A. Grigoryev and A. V. Tsiganov, Symbolic software for separation of variables in the Hamilton-Jacobi equation for the l-systems, Regul. Chaotic Dyn. **10**, 413 (2005).

[29] H. A. Bethe and E. E. Salpeter, *Quantum Mechanics of One-And Two-Electron Atoms* (Springer-Verlag, Berlin, 2012).

[30] H. Suno, L. Andric, T. P. Grozdanov, and R. McCarroll, Photoionization of atoms in parallel electric and magnetic fields: Cross-section calculations using the Lanczos algorithm and the complex coordinate method in a discrete variable representation, Eur. Phys. J. D **13**, 213 (2001).

[31] D. Dimitrovski, T. P. Grozdanov, E. A. Solov'ev, and J. S. Briggs, Ionization and excitation of the hydrogen atom by an electric pulse, J. Phys. B: At., Mol. Opt. Phys. **36**, 1351 (2003).

[32] R. S. Mulliken, The Rydberg states of molecules. 1a parts i-v1b, J. Am. Chem. Soc. **86**, 3183 (1964).

[33] E. So, M. T. Bell, and T. P. Softley, Wave-packet propagation study of the charge-transfer dynamics of Rydberg atoms with metal surfaces, Phys. Rev. A **79**, 012901 (2009).

[34] L. V. Jørgensen, F. Labohm, H. Schut, and A. Van Veen, Evidence of very low-energy positron reflection off tungsten surfaces, J. Phys.: Condens. Matter **10**, 8743 (1998).

[35] S. Hong, C.-S. Lee, M.-H. Lee, Y. Lee, K. Y. Ma, G. Kim, S. I. Yoon, K. Ihm, Ki-Jeong Kim, T. J. Shin *et al.*, Ultralow-dielectric-constant amorphous boron nitride, Nature (London) **582**, 511 (2020).

[36] K. Kajita, A new two-dimensional electron system on the surface of solid neon, Surf. Sci. **142**, 86 (1984).

[37] A. P. Mills, Jr. and E. M. Gullikson, Solid neon moderator for producing slow positrons, Appl. Phys. Lett. **49**, 1121 (1986).

[38] R. G. Greaves and C. M. Surko, Solid neon moderator for positron-trapping experiments, Can. J. Phys. **74**, 445 (1996).

[39] M. E. Fajardo, C. Michael Lindsay, and C. D. Molek, Efficient cryosolid positron moderators, Technical report, Air Force Research Laboratory Munitions Directorate, 2012.

[40] G. W. Ford, L. M. Sander, and T. A. Witten, Lifetime Effects of Positronium in Powders, Phys. Rev. Lett. **36**, 1269 (1976).

[41] L. O. Roellig, M. Weber, S. Berko, B. L. Brown, K. F. Canter, K. G. Lynn, A. P. Mills, S. Tang, and A. Viescas, A positronium beam and positronium reflection from LiF, in *Atomic Physics with Positrons* (Springer-Verlag, Berlin, 1987), pp. 233–239.

[42] A. J. Garner, A. Özen, and G. Laricchia, Positronium beam scattering from atoms and molecules, Nucl. Instrum. Methods Phys. Res., Sect. B **143**, 155 (1998).

[43] M. Weber, S. Tang, R. Khatri, S. Berko, K. F. Canter, K. G. Lynn, A. P. Mills, Jr., L. O. Roellig, and A. J. Viescas in *Proceedings of a workshop, 19-21 July 1989, at NASA Goddard Space Flight Center, Greenbelt, Maryland USA*, edited by Richard J. Drachman, Annihilation in Gases and Galaxies; NASA Conference Publication 3058 (NASA Office of Management, Scientific and Technical Information Division, 1990), p. 137.

[44] A. P. Mills Jr. and M. Leventhal, Can we measure the gravitational free fall of cold Rydberg state positronium? Nucl. Instrum. Methods Phys. Res., Sect. B **192**, 102 (2002).

[45] A. C. L. Jones, J. Moxom, H. J. Rutbeck-Goldman, K. A. Osorno, G. G. Cecchini, M. Fuentes-Garcia, R. G. Greaves, D. J. Adams, H. W. K. Tom, A. P. Mills Jr., and M. Leventhal, Focusing of a Rydberg Positronium Beam with an Ellipsoidal Electrostatic Mirror, Phys. Rev. Lett. **119**, 053201 (2017).

[46] M. Charlton, S. Eriksson, and G. M. Shore, *Antihydrogen and Fundamental Physics*, SpringerBriefs in Physics (Springer, Cham, 2020).